Macromolecules

Article

pubs.acs.org/Macromolecules

Conjugated Copolymers of Vinylene Flanked Naphthalene Diimide

Zhuping Fei,[†] Yang Han,*[,†,‡] Jaime Martin,[§] Fiona H. Scholes,[∥] Mohammed Al-Hashimi,[#] Siham Y. AlQaradawi,[⊥] Natalie Stingelin,[§] Thomas D. Anthopoulos,[‡] and Martin Heeney*[,†]

[†]Department of Chemistry and Centre for Plastic Electronics, [‡]Department of Physics and Centre for Plastic Electronics, and [§]Department of Materials and Centre for Plastic Electronics, Imperial College London, London SW7 2AZ, U.K.

[∥]CSIRO Manufacturing, Private Bag 10, Clayton South, Victoria 3169, Australia

[⊥]Department of Chemistry & Earth Sciences, Qatar University, P.O. Box 2713, Doha, Qatar

[#]Department of Chemistry, Texas A&M University at Qatar, P.O. Box 23874, Doha, Qatar

S *Supporting Information*

ABSTRACT: We report the synthesis of a novel naphthalene diimide (NDI) monomer containing two (tributylstannyl)vinyl groups. The utility of this building block is demonstrated by its copolymerization with five different electron-rich comonomers under Stille conditions. The resulting high molecular weight polymers show red-shifted optical absorptions in comparison to the analogous polymers without the vinylene spacer and a significant increase in the intensity of the low-energy intramolecular charge transfer band. The polymers all exhibit ambipolar behavior in bottom-gate, top-contact organic thin-film transistors. The insertion of a solution-processed barium hydroxide layer between the polymer and the gold electrode led to unipolar behavior with improved electron mobilities.

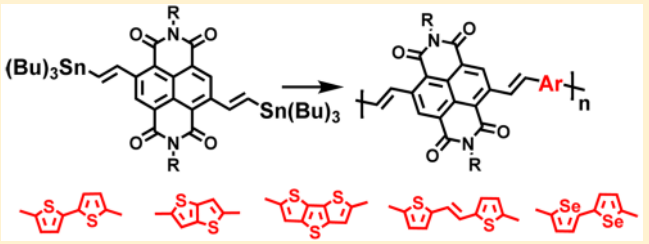

INTRODUCTION

Solution-processed conjugated polymers have attracted widespread interest due to their potential applications in a range of organic electronic devices. Among those polymer-based devices, organic thin-film transistors (OTFTs) are of special interest as the building blocks of circuits for potential use in printed electronic devices and displays.[1,2] Classified by the polarity of the dominant charge carriers in the transistor channel, conjugated polymers are typically categorized as p-type (hole dominant), n-type (electron dominant), or ambipolar (both carriers). Compared to the well-developed p-type polymers, the emergence and development of complementary n-type polymers for OTFTs has been less rapid, with fewer examples reported.[3−8] The n-type organic semiconductors typically contain strongly electron-deficient building blocks in their structures in order to facilitate the injection of electrons as well as to stabilize the resulting negative polaron.[9−13] However, the variety of building blocks with the requisite high electron affinity and solubility to prepare processable n-type conjugated polymers is relatively limited.[3]

One building block that has been extensively investigated is 1,4,5,8-naphthalene diimide (NDI), which is composed of a planar conjugated naphthalene core with two electron-withdrawing diimide groups.[14−16] The imide groups act to both increase the electron affinity of the monomer as well as providing a convenient site for the attachment of the necessary solubilizing side chains. Copolymers of NDI constitute some of the first reported classes of n-type polymers,[17−24] although the transistor performance of early examples was relatively modest. A significant breakthrough was reported by Facchetti and coworkers, who found that the copolymer of NDI and 2,2′-bithiophene, poly{[*N*,*N*′-bis(2-octyldodecyl)naphthalene-1,4,5,8-bis(dicarboximide)-2,6-diyl]-*alt*-5,5′-(2,2′-bithiophene)}(P(NDI2OD-T2)), exhibited an electron mobility up to 0.85 $cm^2\ V^{-1}\ s^{-1}$ in TFT devices.[25] Since then, a variety of NDI-based polymers have been explored by copolymerization of NDI with a range of electron-rich and electron-deficient comonomers in order to adjust the energy levels and polymer microstructure for the purpose of performance improvement.[3,26−34]

Interestingly, a close look at the structure of the repeat unit of P(NDI2OD-T2) by density functional theory (DFT) calculations demonstrates that there is a significant torsion angle between the NDI unit and the adjacent thiophene ring. The reported angle varies from 40° to 47° depending on the specifics of the computation[26,35−38] and has been calculated to reduce to 34° upon stacking of the aromatic backbones.[38] Replacing the adjacent thiophene ring with furan helps to reduce the torsion angle, to somewhere between 20° and 30°.[39] Nevertheless, this is a significant twist which might potentially hamper backbone delocalization and $\pi-\pi$ stacking of the polymer backbones, thereby hindering interchain charge transport. Previously, we found that the introduction of a vinylene group in a polymer backbone could effectively reduce the torsion angle between two adjacent thiophene comonomers, enhancing backbone delocalization and increasing TFT

Received: July 3, 2016
Revised: August 8, 2016

DOI: 10.1021/acs.macromol.6b01423
Macromolecules XXXX, XXX, XXX−XXX

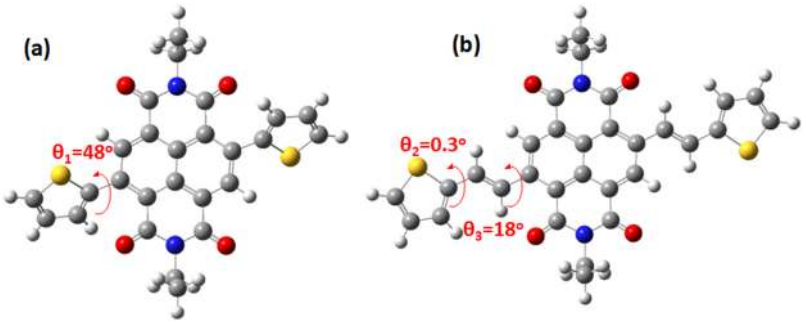

Figure 1. Energy-minimized structures of a methyl-substituted T-NDI-T (a) and T-V-NDI-V-T (b). All calculated using DFT at the B3LYP/6.31G* level.

Scheme 1. Synthetic Route to Monomer and Polymers[a]

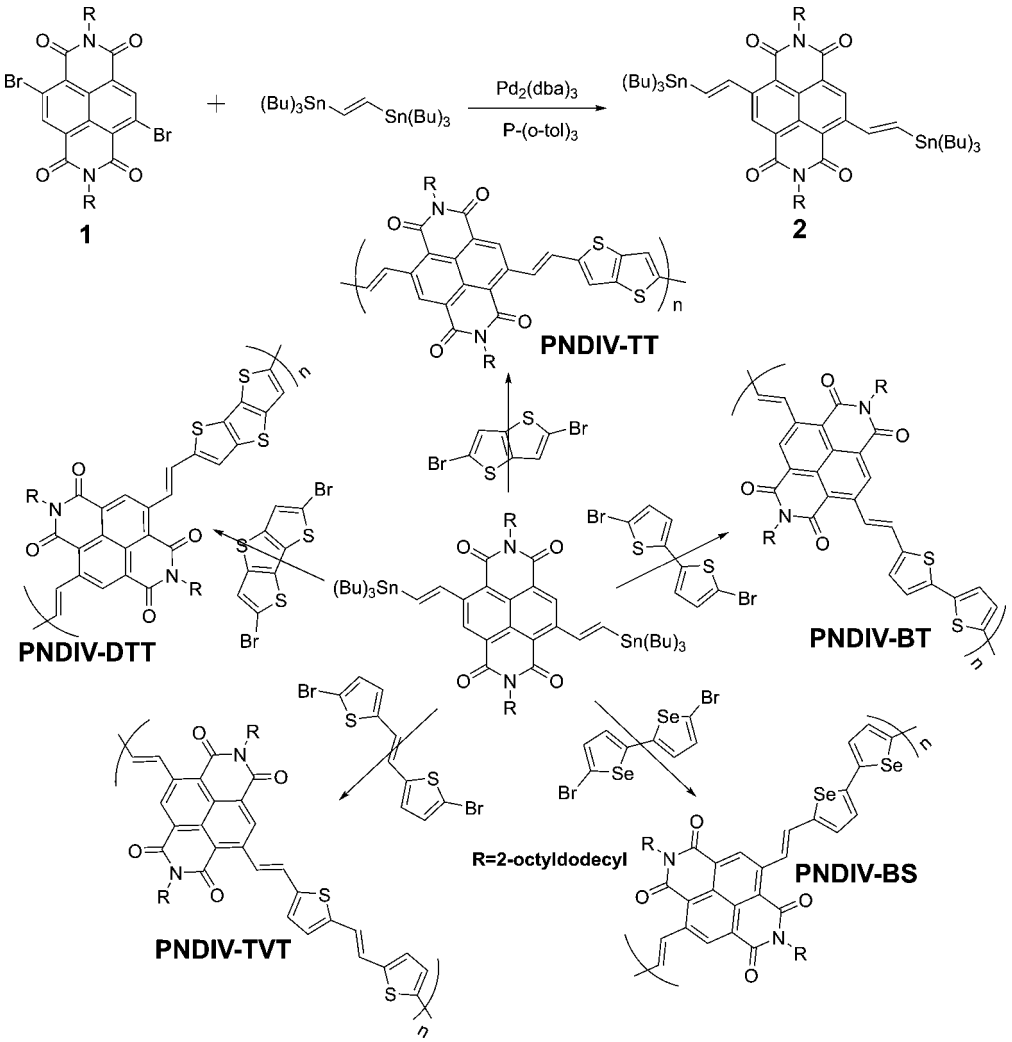

[a]Polymerization conditions were 0.02 equiv of $Pd_2(dba)_3$, 0.08 equiv of $P(o\text{-Tol})_3$, and CB in all cases.

performance.[40,41] Therefore, we were interested to see if a similar strategy could be used to reduce the torsion angle in NDI copolymers. To predict the effect of the vinyl spacer on the twist angle between thiophene and NDI fragments, DFT calculations were performed on thiophene-NDI-thiophene (T-NDI-T) and thiophene-vinyl-NDI-vinyl-thiophene (T-V-NDI-V-T) model systems, and the minimum-energy conformations are shown in Figure 1. The calculations on the T-NDI-T unit agree with the large twist angle previously reported, although in this simple monomeric example the angle is slightly larger than the previous studies which used oligomeric materials. Importantly, the calculations show that insertion of the vinyl spacer between thiophene and NDI significantly reduces the torsional twist predicted.

Following these calculation results, we herein report the preparation of a new NDI-based building block, 2,7-bis(2-octyldodecyl)-4,9-bis((*E*)-2-(tributylstannyl)vinyl)benzo[*lmn*][3,8]-phenanthroline-1,3,6,8(2*H*,7*H*)-tetraone, by a facile

DOI: 10.1021/acs.macromol.6b01423
Macromolecules XXXX, XXX, XXX−XXX

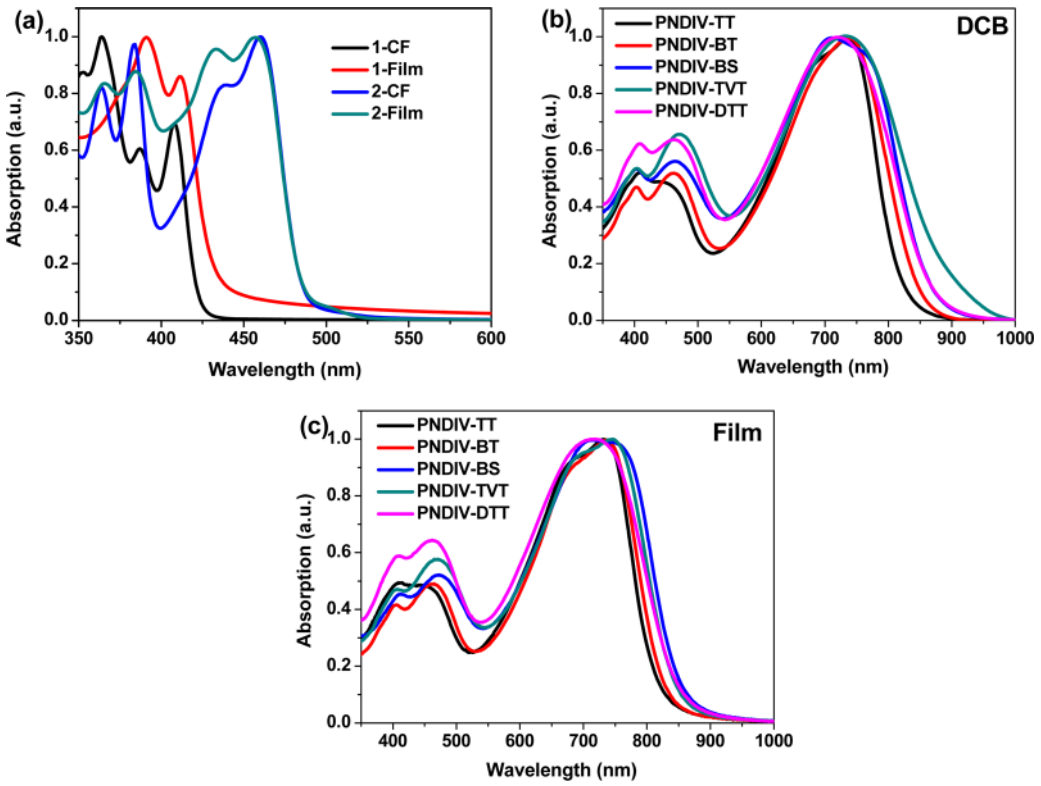

Figure 2. UV−vis absorption spectra of monomer **1** and **2** (a) and PNDIV-TT, PNDIV-BT, PNDIV-BS, PNDIV-TVT, and PNDIV-DTT in dilute *o*-DCB (b) and as spun-cast thin films (c).

Table 1. Physical Properties of PNDIV-TT, PNDIV-BT, PNDIV-BS, PNDIV-TVT, and PNDIV-DTT

polymer	M_n[a] (kDa)	M_w[a] (kDa)	$Đ$	$\lambda_{abs,max}$ (sol) (nm)	$\lambda_{abs,max}$ (film) (nm)	λ_{onset} (film) (nm)	$E_{g,opt}$[b] (eV)	HOMO[c] (eV)	LUMO[d] (eV)
PNDIV-TT	32	78	2.4	406, 455, 699, 736	411, 458, 690, 731	809	1.53	−5.58	−4.05
PNDIV-BT	117	337	2.9	403, 460, 737	405, 463, 736	824	1.50	−5.55	−4.05
PNDIV-BS	20	102	5.1	403, 464, 710, 754	411, 471, 712, 745	850	1.46	−5.50	−4.04
PNDIV-TVT	47	230	4.8	403, 471, 733	405, 470, 701, 746	846	1.48	−5.46	−3.98
PNDIV-DTT	21	51	2.4	408, 464, 720	408, 462, 718	852	1.45	−5.46	−4.01

[a]Measured using gel permeation chromatography (against polystyrene standards) in chlorobenzene at 80 °C. [b]Optical band gap estimated from the low-energy band edge in the optical spectrum. [c]HOMO estimated as the inverse of ionization potential measured by UV-PESA (error ±0.05 eV). [d]LUMO = HOMO + $E_{g,opt}$.

method. We demonstrate its copolymerization with five different donor comonomers by the Stille coupling reaction. We chose five donor comonomers to investigate, partly on the basis that their respective copolymers with NDI have all previously been reported, which facilitates comparison to previous results. Thus, the donor comonomers included 2,2′-bithiophene (BT),[20,24,25,28,42,43] 2,2′-biselenophene (BS),[30] thieno[3,2-*b*]thiophene (TT),[28,34] dithieno[3,2-*b*:2,3-*d*]-thiophene (DTT),[28,34] and thienylene−vinylene−thienylene (TVT).[26,27] Here we report the optoelectronic properties of these novel vinylene-containing copolymers and their behavior in organic thin film transistor devices.

RESULTS AND DISCUSSION

Synthesis and Characterization of Monomer and Polymers. The synthetic route to the monomer and polymers is shown in Scheme 1. Starting material 4,9-dibromo-2,7-bis(2-octyldodecyl)benzo[*lmn*][3,8]phenanthroline-1,3,6,8(2*H*,7*H*)-tetraone (**1**) was synthesized according to the reported method.[27] The key monomer **2** was readily synthesized by palladium-catalyzed Stille coupling of **1** with 4 equiv of commercially available (*E*)-1,2-bis(tributylstannyl)ethene. The product was readily purified by column chromatography over normal phase silica in a good yield of 72%. All polymers were synthesized by Stille coupling of monomer **2** and the appropriate dibromo monomers under reflux conditions in chlorobenzene (CB). The resulting polymers were purified by precipitation and Soxhlet extraction to remove the low-weight oligomers and catalyst residues. PNDIV-TT, PNDIV-BT, PNDIV-BS, PNDIV-TVT, and PNDIV-DTT were obtained as dark green solids in yields of 54−85%. PNDIV-TT and PNDIV-DTT could be dissolved in common solvents such as chloroform and chlorobenzene at room temperature, whereas PNDIV-BT, PNDIV-BS, and PNDIV-TVT were less soluble and could only be dissolved in hot chlorobenzene.

The structures of all polymers were confirmed by a combination of ^{1}H NMR and elemental analysis. The number-average molecular weights (M_n) were measured by gel permeation chromatography (GPC) in hot (80 °C) chlorobenzene against polystyrene standards. PNDIV-TT, PNDIV-BT, PNDIV-BS, PNDIV-TVT, and PNDIV-DTT had a M_n of 32, 117, 20, 47, and 21 kDa, respectively. The dispersity

DOI: 10.1021/acs.macromol.6b01423
Macromolecules XXXX, XXX, XXX−XXX

($Đ$) of the polymers was in the range of 2.4−5.1. We note that the measurements on PNDIV-BT, PNDIV-BS, and PNDIV-TVT were complicated by the reduced solubility and tendency to aggregate in solution, which may explain the relatively high dispersities observed. The thermal stability properties of those polymers were evaluated by thermal gravimetric analysis (TGA) (Figures S1−S5). The polymers all exhibited excellent thermal stability, with a 5% weight loss occurring at temperatures higher than 400 °C in nitrogen, suggesting that the introduction of the vinylene group does not have a detrimental impact on polymer stability.

Optical Properties. The UV−vis absorption spectra of starting material **1** and product monomer **2** in dilute chloroform and as a film are shown in Figure 2a. Compared to that of **1**, the absorption band of **2** was red-shifted from 410 to 460 nm, in both solution and film. This red-shift of the absorption band can be attributed to the extension of the conjugation length by introduction of vinyl group to the main NDI unit. The UV−vis absorption spectra of the polymers in dilute *o*-dichlorobenzene (*o*-DCB) and as thin films are shown in Figures 2b and 2c, with the data summarized in Table 1. All polymers exhibit two main broad absorption bands. The high-energy region (400−500 nm) can be assigned to $\pi-\pi^*$ transitions of the main backbones, while the low-energy region (530−900 nm) can be attributed to intramolecular charge transfer (ICT) from the thiophene or selenophene based electron-rich units to the electron-deficient NDI units. PNDIV-BT exhibits absorption peaks at 403, 460, and 737 nm in solution. These absorption peaks are red-shifted compared to those of P(NDI2OD-T2) in *o*-DCB by ca. 50 nm,[38,44] which can be explained by the extension of the conjugation length of the main backbone by the additional vinyl groups. Although solution comparisons are complicated for the other polymers due to differing solvent systems, in all cases a red-shift of 20−50 nm in λ_{max} is observed for thin films of the NDIV-TT, -DTT, -BS, and -TVT copolymers compared to the their respective NDI copolymers.[26,30,34] In addition, it is clearly apparent that all the vinylene copolymers have much more intense ICT transitions with respect to the high-energy absorption band than their NDI analogues, in both thin film and solution, indicating a more efficient intramolecular charge transfer in the vinylene copolymers. The absorption peaks of polymers in film are similar to those in solution, suggesting the polymers are aggregated even in dilute *o*-DCB. Replacing the donor unit in the backbone does not make a dramatic difference to the maximum absorption wavelength, but it subtly affects the band gap. The absorption onsets of PNDIV-TT, PNDIV-BT, PNDIV-BS, PNDIV-TVT, and PNDIV-DTT in the solid state are 809, 824, 850, 846, and 852 nm, corresponding to the optical band gaps of 1.53, 1.50, 1.46, 1.48, and 1.45 eV, respectively.

The ionization potential (IP) of thin films of PNDIV-TT, PNDIV-BT, PNDIV-BS, PNDIV-TVT, and PNDIV-DTT were measured by photoelectron spectroscopy in air (PESA) to be 5.58, 5.55, 5.50, 5.46, and 5.46 eV, respectively, and the highest occupied molecular orbital (HOMO) was approximated as the negative of the measured IP. The LUMO levels of polymers were estimated to be −4.05, −4.05, −4.04, −3.89, and −4.01 eV, respectively, by subtracting the optical band gap from the measured IPs (see Table 1). We note that this estimation does not account for the exciton binding energy but does allow a comparison among this series of materials. The data suggest that the most noticeable effect of changing the electron-rich donor unit is to influence the HOMO level of the copolymers, whereas the LUMO remains relatively constant throughout the series. We have not attempted to compare the IP of these vinylene copolymers to those reported for the analogous NDI copolymers due to the different measurement techniques used to measure IP.

Structural (X-ray) Characterization. The ordering of thin films of PNDIV-TT, PNDIV-BT, PNDIV-BS, PNDIV-TVT, and PNDIV-DTT was investigated by wide-angle X-ray scattering (WAXS), as shown in Figure 3. Films were prepared

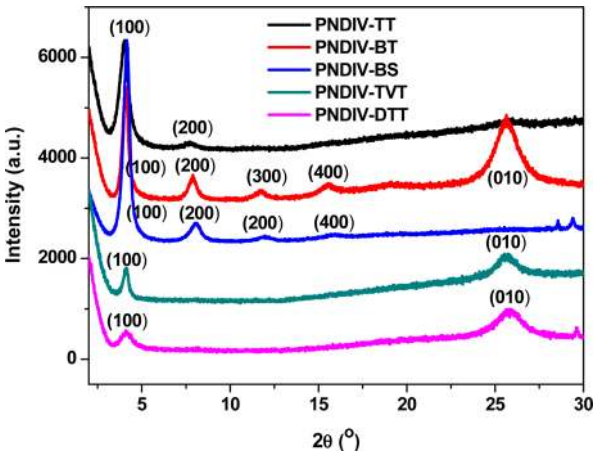

Figure 3. X-ray diffraction patterns of PNDIV-TT, PNDIV-BT, PNDIV-BS, PNDIV-TVT, and PNDIV-DTT drop-cast films after annealed at 300 °C for 30 min under N_2 (offset for clarity).

by drop-casting hot *o*-DCB solutions onto crystalline silicon substrates, followed by annealing at 300 °C for 30 min under N_2. For PNDIV-TT, PNDIV-BT, PNDIV-BS, PNDIV-TVT, and PNDIV-DTT, there is a distinct diffraction peak (100) at 4.02, 4.08, 4.16, 4.12, and 4.12° (2θ) corresponding to an interlayer *d*-spacing of 22.96, 21.64, 21.22, 21.43, and 21.43 Å, respectively. In accordance with earlier studies,[26,27] we attribute this to a lamellar-like packing of the conjugated polymer backbones. The lamellar stacking distances of PNDIV-BT and PNDIV-TVT are shorter than those of their nonvinyl spacer analogues P(NDI2OD-T2) and PNVT 8 with identical side chains,[26] which indicates a denser packing of the polymer backbones along the (x00) direction as a result of the introduction of the vinylene spacer between NDI and thiophene units.[45] PNDIV-TT exhibits the longest lamellar stacking distance among these five polymers, which is possibly related to an increased steric hindrance of side chains on adjacent NDI molecules due to the TT being the shortest aromatic spacer used.[46] Apart from the first-order lamellar stacking peak (100), a progression of peaks up to the fourth order (400) is also observed in the PNDIV-BT and PNDIV-BS films, suggesting that in this direction the structural coherence is more ordered for these two polymers. We note that both of these polymer displayed a tendency to also aggregate in solution, as evident from the high apparent M_w measured by GPC. The films of PNDIV-BT, PNDIV-TVT, and PNDIV-DTT also show a clear diffraction at 25.7, 25.7, and 25.8° (2θ), corresponding to a *d*-spacing of ca. 3.5 Å, respectively, which is likely related to the $\pi-\pi$ stacking distance of the aromatic polymer backbones. The appearance of both lamellar and $\pi-\pi$ peaks for these three polymers suggests they may have a mixture of face-on and edge-on orientation packing with

DOI: 10.1021/acs.macromol.6b01423
Macromolecules XXXX, XXX, XXX−XXX

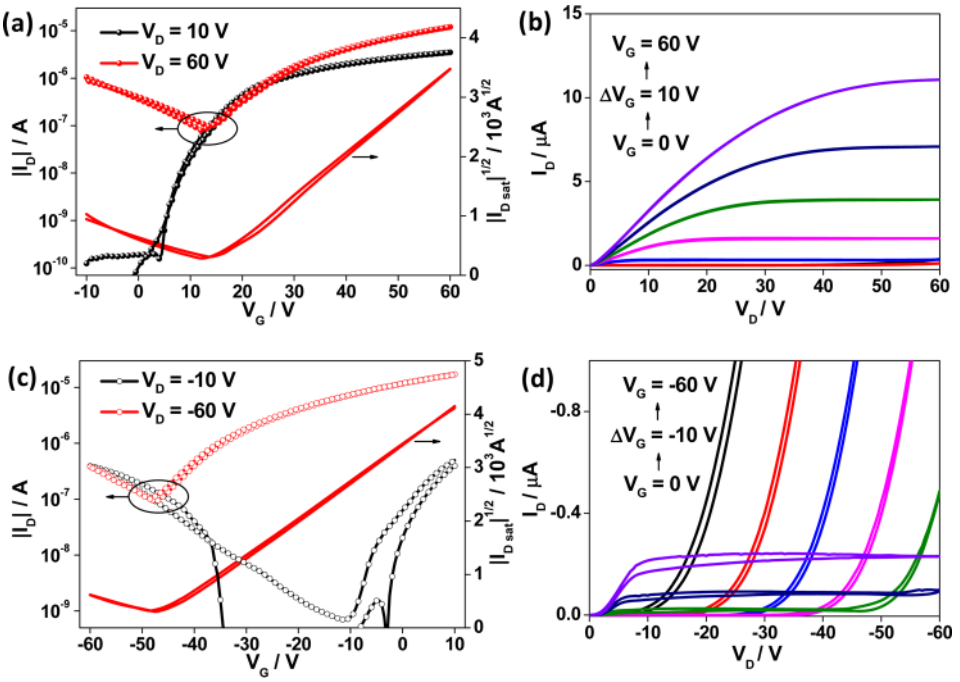

Figure 4. Transfer (a, c) and output (b, d) characteristics of PNDIV-BT-based BG/TC configuration OTFT device under positive and negative bias. The width and length of the transistor channels are W = 1000 μm and L = 40 μm, respectively.

Table 2. Summary of OTFT Performance of Devices of PNDIV-TT, PNDIV-BT, PNDIV-BS, PNDIV-TVT, and PNDIV-DTT in Bottom-Gate Top-Contact Configuration

	electron				hole			
polymer	$\mu_{e,sat\ ay}$ ($\mu_{e,sat\ max}$) [cm^2 V^{-1} s^{-1}]	$\mu_{e,lin}$ [cm^2 V^{-1} s^{-1}]	V_{th} [V]	V_{on}/V_{off}	$\mu_{h,sat}$ ($\mu_{h,sat\ max}$) [cm^2 V^{-1} s^{-1}]	$\mu_{h,lin}$ [cm^2 V^{-1}s^{-1}]	V_{th} [V]	I_{on}/I_{off}
PNDIV-TT	0.008 ± 0.001 (0.009)	0.009 ± 0.0008	25.7 ± 0.8	(2−3) × 10^2	0.0001 ± 0.00001 (0.0001)	0.00005 ± 0.00001	−44.0 ± 2.1	<10
PNDIV-BT	0.05 ± 0.004 (0.06)	0.03 ± 0.009	11.9 ± 0.9	(1−2) × 10^2	0.008 ± 0.003 (0.009)	0.007 ± 0.004	−32.5 ± 3.7	<10
PNDIV-BS	0.02 ± 0.001 (0.02)	0.01 ± 0.003	27.6 ± 2.9	(9−10) × 10	0.0008 ± 0.0003 (0.001)	0.0008 ± 0.0002	−42.3 ± 3.1	<10
PNDIV-TVT	0.04 ± 0.002 (0.04)	0.016 ± 0.003	26.6 ± 0.6	(1−2) × 10^2	0.009 ± 0.0009 (0.01)	0.004 ± 0.0005	−30.5 ± 2.4	(1−2) × 10^2
PNDIV-DTT	0.01 ± 0.0003 (0.01)	0.01 ± 0.0006	18.7 ± 0.3	(1−2) × 10^2	0.002 ± 0.0002 (0.002)	0.0008 ± 0.0003	−44.6 ± 0.7	<10

respect to the substrate. To the best of our knowledge, 3.5 Å is the shortest π−π stacking distance reported for a NDI-based polymer and suggests that the reduction of backbone torsion by the introduction of a vinyl spacer may help to facilitate packing of the conjugated backbones. Despite the evidence of thin film crystallinity, we could see no evidence for a backbone melt for PNDIV-BT by differential scanning calorimetry (DSC), even heating above the decomposition temperature to 450 °C using flash DSC (Figure S6, with a heating/cooling rate of 500 °C s^{-1}). We note that the backbone melt of PNDIV-BT appears to therefore be significantly higher than that of the analogous nonvinylene polymer P(NDI2OD-T2), which is around 320 °C,[47] as would be expected for a more coplanar backbone.

OTFT Characterization. The electrical properties of all polymers were studied using electrical field-effect measurements at room temperature under inert atmosphere. For this purpose bottom gate, top contact (BG/TC) OTFTs were fabricated and used throughout this study. All devices were fabricated by spin-casting from 10 mg/mL *o*-DCB solution onto Si/SiO_2 substrates pretreated with trichloro(octadecyl)-silane (OTS). As-spun films were then dried and further annealed at 300 °C for 30 min followed by the deposition of the Au source/drain electrodes via vacuum sublimation. High-temperature postannealing was employed since it has previously been shown to promote electron transport via the reduction of electron traps.[48] We also performed a preliminary investigation the effect of annealing temperature on PNDIV-BT, using annealing temperatures of 100, 200, and 300 °C. The transfer characteristics in the saturation regime are shown in Figure S7, and the mobility and threshold parameters against temperature are plotted in Figure S8. The best device performance was observed at 300 °C, and as such this was the temperature chosen to investigate all polymers.

Figure 4 and Figures S9−S12 show the transfer characteristics of all five polymers under positive gate bias (V_G). As can be seen, all polymers exhibited ambipolar transfer characteristics with a dominant electron transporting character. This characteristic ambipolar behavior is not surprising from the polymer energy levels and is most likely attributed to the work function of the Au electrodes (~5.0 eV), which enables injection of both holes and electrons into the HOMO and

DOI: 10.1021/acs.macromol.6b01423
Macromolecules XXXX, XXX, XXX−XXX

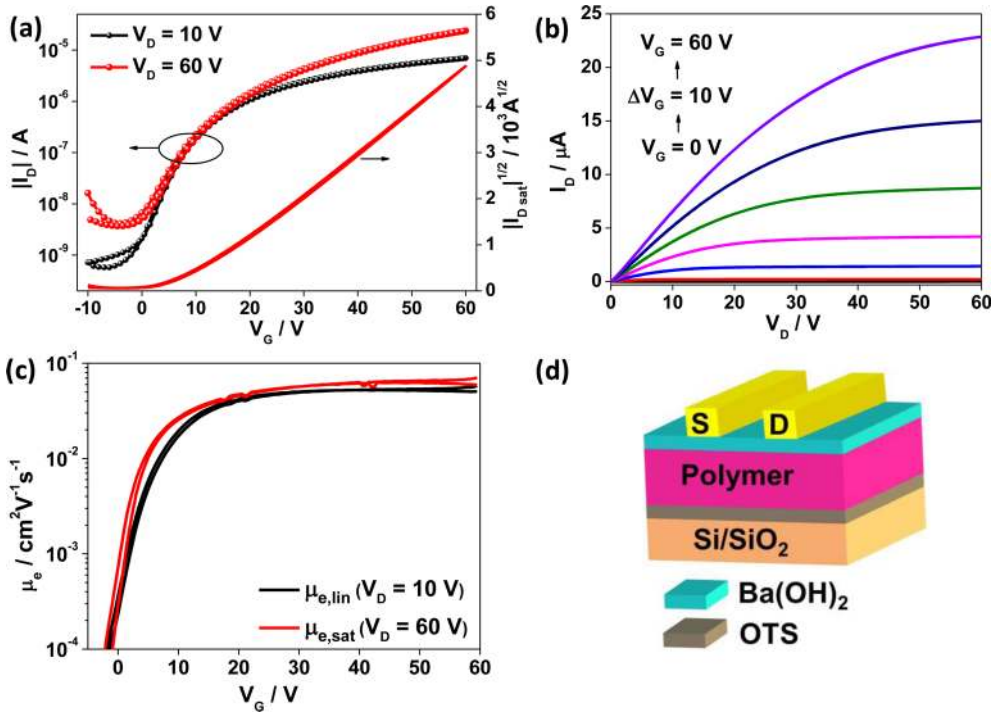

Figure 5. Transfer (a) and output (b) characteristics of PNDIV-BT-based BG/TC configuration OTFT device with $Ba(OH)_2$ layer between polymer and Au electrode. (c) Mobility calculation based on first derivative of the linear regime transfer curve and first derivative of the square root of the saturation regime transfer curve. (d) Transistor device configuration. The width and length of the transistor channels are W = 1000 μm and L = 40 μm, respectively.

Table 3. Summary of OTFT Performance of Devices of PNDIV-TT, PNDIV-BT, PNDIV-BS, PNDIV-TVT, and PNDIV-DTT in Bottom-Gate Top-Contact Configuration with $Ba(OH)_2$ Layer between Polymer and Au Electrode

polymer	$\mu_{e,sat\,av}$ [cm^2 V^{-1} s^{-1}]	$\mu_{e,lin\,av}$ [cm^2 V^{-1} s^{-1}]	V_{th} [V]	I_{on}/I_{off}
PNDIV-TT	0.03 ± 0.00082	0.024 ± 0.0013	12.7 ± 1.1	(2−3) × 10^3
PNDIV-BT	0.07 ± 0.0029	0.056 ± 0.0013	8.1 ± 0.6	(6−7) × 10^3
PNDIV-BS	0.02 ± 0.0044	0.019 ± 0.0022	15.5 ± 0.9	(1−2) × 10^3
PNDIV-TVT	0.04 ± 0.0019	0.025 ± 0.0022	10.9 ± 0.5	(8−9) × 10^2
PNDIV-DTT	0.02 ± 0.0031	0.017 ± 0.0017	13.9 ± 0.5	(5−6) × 10^3

LUMO, respectively.[49,50] The various transistor parameters extracted from these measurements are summarized in Table 2.

Comparing between materials, the electron mobility varies by less than 1 order of magnitude for all polymers, suggesting that the choice of donor has a relatively small impact on the device performance (Table 2). Among the polymers studied, PNDIV-BT exhibited the highest electron mobility, with a maximum value of 0.06 cm^2 V^{-1} s^{-1}, which may relate to its more ordered microstructure and high tendency to aggregate as discussed above. With the exception of PNDIV-BT-based OTFTs, all devices exhibited large threshold voltages (V_{th}), suggesting a significant injection barrier, as expected from the work function of the Au electrode. Although all polymers exhibited ambipolar transport behavior, the hole mobility values extracted are significantly lower than those of electrons for all five polymers studied. To this end, significant carrier injection issues are evident and are most likely at least partly responsible for the high threshold voltages observed. This highly unbalanced ambipolar behavior results in the relatively low current I_{on}/I_{off} ratios that are typically in the range of ~10^2.

In an effort to suppress hole transport and obtain pure unipolar n-type transistor behavior, we investigated the incorporation of a thin layer of barium hydroxide ($Ba(OH)_2$) between the polymer semiconductor film and Au S/D electrodes. $Ba(OH)_2$ has previously been shown to be useful as solution-processed electrode modifier for the purpose of enhancing electron injection.[51] Depositing $Ba(OH)_2$ onto bottom contact Au electrodes prior to semiconductor deposition was shown to modify the work function to ca. 3.5 eV, facilitating electron injection into the LUMO of P(NDI2OD-T2) and suppressing hole injection into the HOMO compared to unmodified Au. In our case methanolic solutions of $Ba(OH)_2$ were drop-cast directly onto the annealed polymer film prior to the evaporation of Au contacts. Gratifyingly, the addition of the $Ba(OH)_2$ interlayer significantly improved the transistor characteristics (Figure 5 and Figures S13−S16), with all polymers exhibiting strictly unipolar n-type transport characteristics. Noteworthy is the fact that the operating hysteresis observed between forward and reverse scans is negligible. The transistor parameters extracted from these measurements are summarized in Table 3. Importantly, insertion of $Ba(OH)_2$ was found to enhance the device performance of all polymers, with PNDIV-BT again showing the highest electron mobility of 0.07 cm^2 V^{-1} s^{-1}. Similarly, the threshold voltage in all polymer OTFTs reduces by more than 10 V, suggesting that the injection barrier for electrons is the main source of the large threshold voltages observed in the polymer OTFTs without $Ba(OH)_2$. The on-current of all

DOI: 10.1021/acs.macromol.6b01423
Macromolecules XXXX, XXX, XXX−XXX

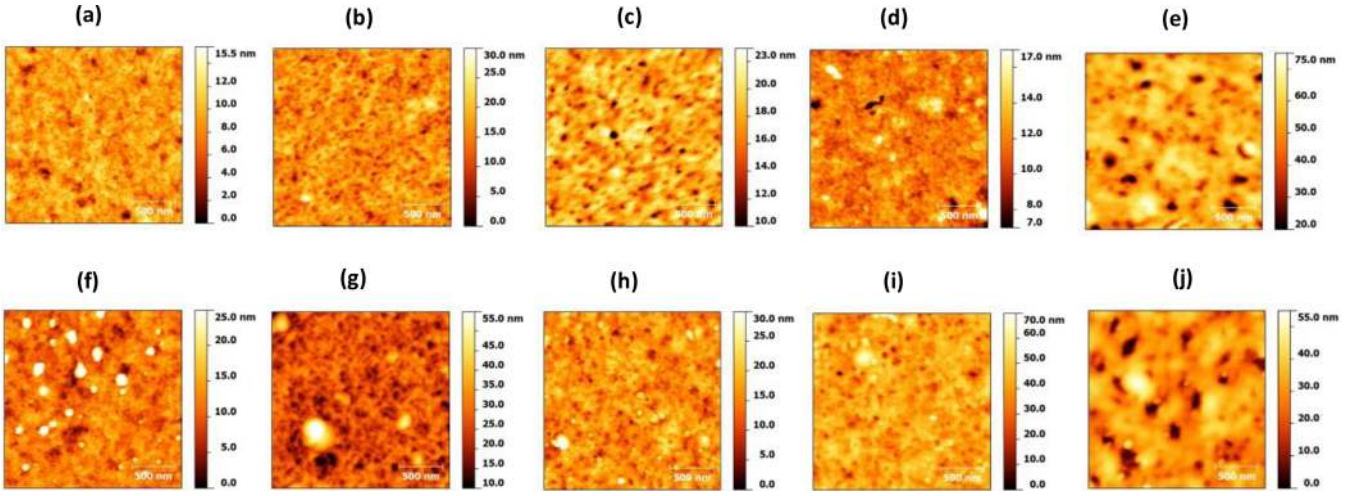

Figure 6. Topography images of PNDIV-TT, PNDIV-BT, PNDIV-BS, PNDIV-TVT, and PNDIV-DTT in bottom-gate top-contact configuration without $Ba(OH)_2$ layer (a–e) and with $Ba(OH)_2$ layer (f–j) between polymer and Au electrodes.

$Ba(OH)_2$-modified devices is found to increase, which together with the reduced off-current results in a significantly increased channel I_{on}/I_{off} ratio by up to 50 times. Although the use of the injection layer only results in a modest increase in electron mobility, we note that the transistors now exhibit close to ideal behavior.[52] In particular, the extracted mobility based on the first derivative of the linear regime transfer curve and first derivative of the square root of the saturation regime transfer curve is almost gate voltage-independent (Figure 5c), in excellent agreement with the gradual channel approximation model employed.[52]

We note that as a control experiment, methanol was drop-cast onto the annealed PNDIV-BT film prior to the evaporation of Au electrodes to investigate the influence of methanol on the performance of transistors while using methanolic solution of $Ba(OH)_2$. As shown in Figure S17, posttreatment with methanol alone gave no obvious hole blocking/electron enhancing effect. We conclude therefore that the improvement of device performance was due to the presence of $Ba(OH)_2$.

Film Morphology. Atomic force microscopy (AFM) was employed to probe the surface morphology of the thin films, both before and after treatment with $Ba(OH)_2$. To accurately reflect the surface states of the polymers in transistors, AFM samples were prepared via identical procedures to the devices, except that no top contacts were evaporated. The AFM images of these polymer films are shown in Figure 6 and Figure S18. PNDIV-TT, PNDIV-BT, PNDIV-BS, and PNDIV-TVT all formed continuous and smooth films on OTS-modified SiO_2 substrates, with root-mean-square surface roughness (RMS) of 1.66, 3.16, 1.87, and 1.27 nm, respectively. PNDIV-DTT, however, formed films with more pin holes and hence obviously higher roughness of 8.00 nm, which may account for the slightly reduced OTFT performance. To determine whether the pin holes were formed due to the high annealing temperature (300 °C), a PNDIV-DTT film annealed at a lower temperature of 100 °C for 2 min was investigated. As shown in Figure S19, those pin holes were already developed at low temperature and likely form during the coating process. Hence, increasing the annealing temperature to 300 °C improved the performance of transistors without introducing extra pin holes.

In all cases the films appear composed of fibrillar networks at the nanometer scale, similar to some other NDI-containing polymers described in the literature.[34,43,45] After the surface treatment with methanolic $Ba(OH)_2$, clear particles were observed on the surface of the annealed polymer, with length scales up to tens of nanometers. Surface roughness increased accordingly to 3.99, 5.83, 3.39, and 6.78 nm for PNDIV-TT, PNDIV-BT, PNDIV-BS, and PNDIV-TVT, respectively. Though the surface roughness remained similar after drop-casting of $Ba(OH)_2$ on PNDIV-DTT film, salt particles were clearly observed in both topography and phase images. In all cases, the underlying film structure did not appear significantly different after deposition of $Ba(OH)_2$ interlayer.

CONCLUSIONS

In summary, we have reported a simple and readily scalable synthesis for the preparation of a new NDI monomer flanked by two vinyl stannyl groups. A series of five copolymers comprising this novel monomer and different thiophene or selenophene based donor units were synthesized and characterized. Soluble polymers of high molecular weight were obtained by the Stille coupling reaction in all cases. In comparing the optical properties of the new vinylene copolymers to the previously reported analogues without the vinylene spacer, the most apparent effect was a red-shift of λ_{max} and a significant increase in the intensity of the low-energy intramolecular charge transfer absorption in comparison to the high-energy absorption. The choice of donor comonomer was shown to have only a subtle effect on the polymer energetics. All polymers exhibited ordered packing in the solid states with PNDIV-BT, PNDIV-TVT, and PDNIV-DTT exhibiting close $\pi-\pi$ stacking distances of 3.5 Å, which are shorter than those reported for analogous NDI-based polymers. These polymers exhibit ambipolar behavior in bottom-gate, top-contact OTFT devices. The insertion of a solution processed $Ba(OH)_2$ layer between the polymer and the gold electrode led to unipolar behavior with improved electron mobilities. Among these polymers, PDNIT-BT exhibited the highest electron mobility of 0.07 $cm^2\ V^{-1}\ s^{-1}$, which we attribute to its enhanced packing structure. In general, the combination of good electron mobility and enhanced optical absorption in the near-IR region might make these polymers interesting candidates for solar cell applications.

DOI: 10.1021/acs.macromol.6b01423
Macromolecules XXXX, XXX, XXX–XXX

EXPERIMENTAL SECTION

General. All reactions were carried out under Ar using solvents and reagents as commercially supplied, unless otherwise stated. 4,9-Dibromo-2,7-bis(2-octyldodecyl)benzo[*lmn*][3,8]phenanthroline-1,3,6,8(2*H*,7*H*)-tetraone (**1**), 2,5-dibromothieno[3,2-*b*]thiophene, 5,5′-dibromo-2,2′-bithiophene, 5,5′-dibromo-2,2′-biselenophene, (*E*)-1,2-bis(5-bromothiophen-2-yl)ethane, and 2,6-dibromodithieno[3,2-*b*:2′,3′-*d*]thiophene were synthesized by the reported methods.

^{1}H and ^{13}C NMR spectra were recorded on a Bruker AV-400 (400 MHz), using the residual solvent resonance of $CDCl_3$ or d_2-1,1,2,2-tetrachloroethane and are given in ppm. Number-average (M_n) and weight-average (M_w) molecular weight were determined by Agilent Technologies 1200 series GPC running in chlorobenzene at 80 °C, using two PL mixed B columns in series, and calibrated against narrow polydispersity polystyrene standards. Flash DSC was performed on a Mettler Toledo Flash DSC 1 at a scan rate of 500 K s $^{-1}$. Thermogravimetric analysis (TGA) was carried out using a PerkinElmer Pyris 1 TGA machine, with heating from 25 to 700 °C at a heating rate of 10 °C/min under N_2. UV−vis spectra were recorded on a UV-1601 Shimadzu UV−vis spectrometer. Flash chromatography was performed on silica gel (Merck Kieselgel 60 F254 230−400 mesh). Photoelectron spectroscopy in Air (PESA) measurements were recorded with a Riken Keiki AC-2 PESA spectrometer with a power setting of 5 nW and a power number of 0.5. Samples for PESA were prepared on glass substrates by spin-coating. X-ray diffraction (XRD) measurements were carried out with a Panalytical X′Pert-pro MRD diffractometer equipped with a nickel-filtered Cu Kα source and X′Celerator detector, using current I = 40 mA and accelerating voltage V = 40 kV. Samples were prepared by drop-casting on silicon substrates. Atomic force microscope (AFM) images were obtained with a Picoscan PicoSPM LE scanning probe in tapping mode. Samples were prepared following the same procedures for fabrication of transistors, except that Au contacts were not applied. DFT calculations were modeled using Gaussian at the B3LYP/6-31G* level. The side chains were modified to methyl groups in order to simplify the calculations.

OTFT (Organic Field Effect Transistor) Device Fabrication. Bottom gate/top contact devices were fabricated on heavily doped n$^+$-Si (100) wafers with 400 nm thick thermally grown SiO_2. The Si/SiO_2 substrates were cleaned using acetone, Decan-90, deionized water, and isopropanol for 15 min under sonication. The nitrogen blow dried substrates were then treated with UV-ozone for 15 min and immersed in trichloro(octadecyl)silane (OTS) solution in anhydrous toluene (1/1000 v/v) overnight to form a self-assembled monolayer before deposition of polymers. The modified substrates were then immersed in clean toluene under mild sonication, followed by rinsing with acetone to remove excess and physically absorbed OTS. Polymers were dissolved in *o*-dichlorobenzene (10 mg/mL) and spin-cast at 2000 rpm for 60 s before being annealed at 300 °C for 30 min. Au (40 nm) source and drain electrodes were deposited onto the polymer film under vacuum through shadow masks. The channel width and length of the transistors are 1000 and 40 μm, respectively, unless otherwise specified. Transistor characterization was carried out under nitrogen using a Keithley 4200 parameter analyzer. Linear mobility was calculated according to the equation

$$\mu_{lin} = \frac{1}{WC_iV_D}\left(\frac{\partial I_D lin}{\partial V_G}\right)$$

and saturation mobility was extracted from the slope of $I_D^{1/2}$ vs V_G:

$$\mu_{sat} = \frac{2L}{WC_i}\left(\frac{\partial \sqrt{I_D sat}}{\partial V_G}\right)^2$$

For transistors with $Ba(OH)_2$ hole blocking layer, polymer solutions were spin-cast onto OTS modified substrates and annealed following the above procedures. 250 μL of $Ba(OH)_2$ solution in methanol (0.1 mg/mL) was drop-cast on the polymer films (2 × 2 cm^2) and dried at 50 °C for 10 min. Au source and drain contacts were then evaporated as mentioned above.

2,7-Bis(2-octyldodecyl)-4,9-bis((E)-2-(tributylstannyl)vinyl)benzo-[lmn][3,8]phenanthroline-1,3,6,8(2H,7H)-tetraone (2). 4,9-Dibromo-2,7-bis(2-octyldodecyl)benzo[*lmn*][3,8]phenanthroline-1,3,6,8-(2*H*,7*H*)-tetraone (**1**) (2.0 g, 2.0 mmol), (*E*)-1,2-bis(tributylstannyl)-ethane (4.9 g, 8.0 mmol), $Pd_2(dba)_3$ (93 mg, 0.1 mmol), and P-(*o*-tol)$_3$ (120 mg, 0.4 mmol) were added into an oven-dried two-neck flask under Ar. Degassed anhydrous toluene (200 mL) was added, and the mixture was heated at 90 °C overnight. The mixture was allowed to cool to room temperature and eluted through a 5 cm thick silicon/KF (4/1, w/w) plug with DCM. The solvent was removed, and the residue was purified by chromatography (eluent: DCM/hexane = 1:2) to afford **2** as a yellow oil (2.1 g, yield: 72%). ^{1}H NMR ($CDCl_3$, 400 MHz) δ (ppm): 8.94 (s, 2H), 8.39 (d, J = 19.5 Hz, 2H), 7.36 (d, J = 19.5 Hz, 2H), 4.13 (*d*, J = 7.2 Hz, 4H), 2.01−1.92 (m, 2H), 1.72−1.56 (m, 12H), 1.43−1.16 (m, 76H), 1.08 (m, 12H), 0.94 (t, J = 7.3 Hz, 18H), 0.88−0.83 (m, 12H). ^{13}C NMR ($CDCl_3$, 100 MHz), δ (ppm): 163.8, 144.5, 143.7, 142.2, 132.3, 126.9, 125.7, 120.0, 44.8, 36.6, 31.9, 30.1, 29.7, 29.4, 29.3, 29.1, 27.4, 26.5, 22.7, 14.1, 13.8, 10.0.

Polymer Synthesis. *Poly{(E)-2,7-bis(2-octyldodecyl)-4-(2-(thieno[3,2-b]thiophen-2-yl)vinyl)-9-vinylbenzo[lmn][3,8]-phenanthroline-1,3,6,8(2H,7H)-tetraone} (PNDIV-TT).* Compound **2** (134.4 mg, 0.092 mmol), 2,5-dibromothieno[3,2-*b*]thiophene (27.5 mg, 0.092 mmol), $Pd_2(dba)_3$ (1.8 mg, 0.0019 mmol), and P-(*o*-tol)$_3$ (2.3 mg, 0.0076 mmol) were added into an overdried 20 mL high-pressure microwave reactor tube. The tube was sealed and flushed with Ar, and then degassed chlorobenzene (4 mL) was added. The mixture was thoroughly degassed under Ar, and then the argon inlet was removed. Then the tube was heated to 140 °C (oil bath) and stirred for 1 day. Tributyl(thiophen-2-yl)stannane (10 μL) and 2-bromothiophene (10 μL) were added successively at a time interval of 4 h to end-cap the end groups, respectively. The polymer was precipitated in methanol (100 mL) and filtered through a Soxhlet thimble. The polymer was extracted using Soxhlet apparatus with methanol, acetone, hexane, and chloroform. The chloroform solution was concentrated *in vacuo* and reprecipitated into methanol. Vacuum filtration followed by drying under vacuum afforded PNDIV-TT as a dark-green solid (80 mg, yield: 85%). ^{1}H NMR (1,1,2,2-tetrachloroethane-d_4, 130 °C, 400 MHz), δ (ppm): 8.55 (broad, 4H), 7.28 (broad, 4H), 4.32 (broad, 4H), 2.15 (broad, 2H), 1.43−1.35 (broad, 64H), 0.95 (broad, 12H). Anal. Calcd $(C_{64}H_{90}N_2O_4S_2)_n$: C, 75.69; H, 8.93; N, 2.76. Found: C, 75.48; H, 9.01; N, 2.71.

Poly{(E)-4-(2-([2,2′-bithiophen]-5-yl)vinyl)-2,7-bis(2-octyldodecyl)-9-vinylbenzo[lmn][3,8]phenanthroline-1,3,6,8(2H,7H)-tetraone} (PNDIV-BT). PNDIV-BT was prepared as described for PDNIV-TT above using compound **2** (138.2 mg, 0.094 mmol), 5,5′-dibromo-2,2′-bithiophene (30.7 mg, 0.094 mmol), $Pd_2(dba)_3$ (1.8 mg, 0.0019 mmol), and P-(*o*-tol)$_3$ (2.3 mg, 0.0076 mmol). The crude polymer was extracted using Soxhlet apparatus with methanol, acetone, hexane, chloroform, and chlorobenzene. The chlorobenzene solution was concentrated *in vacuo* and reprecipitated into methanol. Vacuum filtration followed by drying under vacuum afforded PNDIV-BT as a dark-green solid (72 mg, yield: 73%). ^{1}H NMR (1,1,2,2-tetrachloroethane-d_4, 130 °C, 400 MHz), δ (ppm): 8.52 (broad, 4H), 7.13 (broad, 6H), 4.28 (broad, 4H), 2.17 (broad, 2H), 1.43−1.35 (broad, 64H), 0.95 (broad, 12H). Anal. Calcd $(C_{66}H_{92}N_2O_4S_2)_n$: C, 76.11; H, 8.90; N, 2.69. Found: C, 75.95; H, 9.13; N, 2.80.

Poly{(E)-4-(2-([2,2′-biselenophen]-5-yl)vinyl)-2,7-bis(2-octyldodecyl)-9-vinylbenzo[lmn][3,8]phenanthroline-1,3,6,8(2H,7H)-tetraone} (PNDIV-BS). PNDIV-BS was prepared as described for PDNIV-TT using compound **2** (129.2 mg, 0.089 mmol), 5,5′-dibromo-2,2′-biselenophene (37.1 mg, 0.089 mmol), $Pd_2(dba)_3$ (1.7 mg, 0.0018 mmol), and P-(*o*-tol)$_3$ (2.2 mg, 0.0072 mmol). The crude polymer was extracted using Soxhlet apparatus with methanol, acetone, hexane, chloroform, and chlorobenzene. The chlorobenzene solution was concentrated *in vacuo* and reprecipitated into methanol. Vacuum filtration followed by drying under vacuum afforded PNDIV-BS as a dark-green solid (65 mg, yield: 64%). ^{1}H NMR (1,1,2,2-tetrachloroethane-d_4, 130 °C, 400 MHz), δ (ppm): 8.62 (broad, 4H), 7.28

DOI: 10.1021/acs.macromol.6b01423
Macromolecules XXXX, XXX, XXX−XXX

(broad, 6H), 4.27 (broad, 4H), 2.15 (broad, 2H), 1.43−1.35 (broad, 64H), 0.95 (broad, 12H). Anal. Calcd $(C_{66}H_{92}N_2O_4Se_2)_n$: C, 69.82; H, 8.17; N, 2.47. Found: C, 68.04; H, 8.35; N, 2.58.

Poly{2,7-bis(2-octyldodecyl)-4-((E)-2-(5-((E)-2-(thiophen-2-yl)-vinyl)thiophen-2-yl)vinyl)-9-vinylbenzo[lmn][3,8]phenanthroline-1,3,6,8(2H,7H)-tetraone} (PNDIV-TVT). PNDIV-TVT was prepared as described for PDNIV-TT using compound **2** (136.4 mg, 0.093 mmol), (*E*)-1,2-bis(5-bromothiophen-2-yl)ethane (32.8 mg, 0.093 mmol), $Pd_2(dba)_3$ (1.8 mg, 0.0019 mmol), and P-(*o*-tol)$_3$ (2.3 mg, 0.0076 mmol). The crude polymer was extracted using a Soxhlet apparatus with methanol, acetone, hexane, chloroform, and chlorobenzene. The chlorobenzene solution was concentrated *in vacuo* and reprecipitated into methanol. Vacuum filtration followed by drying under vacuum afforded PNDIV-TVT as a dark-green solid (70 mg, yield: 70%). ^{1}H NMR (1,1,2,2-tetrachloroethane-d_4, 130 °C, 400 MHz), δ (ppm): 8.62 (broad, 4H), 7.03 (broad, 8H), 4.27 (broad, 4H), 2.17 (broad, 2H), 1.43−1.35 (broad, 64H), 0.95 (broad, 12H). Anal. Calcd $(C_{68}H_{94}N_2O_4S_2)_n$: C, 76.50; H, 8.87; N, 2.62. Found: C, 75.30; H, 9.03; N, 3.32.

Poly{2,7-bis(2-octyldodecyl)-4-((E)-2-(5-((E)-2-(thiophen-2-yl)-vinyl)thiophen-2-yl)vinyl)-9-vinylbenzo[lmn][3,8]phenanthroline-1,3,6,8(2H,7H)-tetraone} (PNDIV-DTT). PNDIV-DTT was prepared as described for PDNIV-TT using compound **2** (137.5 mg, 0.094 mmol), 2,6-dibromodithieno[3,2-*b*:2′,3′-*d*]thiophene (33.4 mg, 0.094 mmol), $Pd_2(dba)_3$ (1.8 mg, 0.0019 mmol), and P-(*o*-tol)$_3$ (2.3 mg, 0.0076 mmol). The crude polymer was extracted using a Soxhlet apparatus with methanol, acetone, hexane, and chloroform. The chloroform solution was concentrated *in vacuo* and reprecipitated into methanol. Vacuum filtration followed by drying under vacuum afforded PNDIV-DTT as a dark-green solid (55 mg, yield: 54%). ^{1}H NMR (1,1,2,2-tetrachloroethane-d_4, 130 °C, 400 MHz), δ (ppm): 8.62 (broad, 4H), 7.33 (broad, 4H), 4.30 (broad, 4H), 2.17 (broad, 2H), 1.43−1.35 (broad, 64H), 0.95 (broad, 12H). Anal. Calcd $(C_{66}H_{90}N_2O_4S_3)_n$: C, 73.97; H, 8.47; N, 2.61. Found: C, 73.01; H, 8.82; N, 2.65.

■ ASSOCIATED CONTENT

Supporting Information

The Supporting Information is available free of charge on the ACS Publications website at DOI: 10.1021/acs.macromol.6b01423.

Figures S1−S30 (PDF)

■ AUTHOR INFORMATION

Corresponding Authors

*E-mail: m.heeney@imperial.ac.uk (M.H.).
*E-mail: yang.han@imperial.ac.uk (Y.H.).

Notes

The authors declare no competing financial interest.

■ ACKNOWLEDGMENTS

This work was made possible by a NPRP award [NPRP 6-452-1-089] from the Qatar National Research Fund (a member of The Qatar Foundation). The statements made herein are solely the responsibility of the authors.

■ REFERENCES

(1) Klauk, H. Organic Thin-Film Transistors. *Chem. Soc. Rev.* **2010**, *39*, 2643−2666.

(2) Arias, A. C.; MacKenzie, J. D.; McCulloch, I.; Rivnay, J.; Salleo, A. Materials and Applications for Large Area Electronics: Solution-Based Approaches. *Chem. Rev.* **2010**, *110*, 3−24.

(3) Guo, X.; Facchetti, A.; Marks, T. J. Imide- and Amide-Functionalized Polymer Semiconductors. *Chem. Rev.* **2014**, *114*, 8943−9021.

(4) Kang, I.; Yun, H.; Chung, D. S.; Kwon, S.; Kim, Y. Record High Hole Mobility in Polymer Semiconductors via Side-Chain Engineering Record High Hole Mobility in Polymer Semiconductors via Side-Chain Engineering. *J. Am. Chem. Soc.* **2013**, *135*, 14896−14899.

(5) Holliday, S.; Donaghey, J. E.; McCulloch, I. Advances in Charge Carrier Mobilities of Semiconducting Polymers Used in Organic Transistors. *Chem. Mater.* **2014**, *26*, 647−663.

(6) Tseng, H. R.; Phan, H.; Luo, C.; Wang, M.; Perez, L. A.; Patel, S. N.; Ying, L.; Kramer, E. J.; Nguyen, T. Q.; Bazan, G. C.; Heeger, A. J. High-Mobility Field-Effect Transistors Fabricated with Macroscopic Aligned Semiconducting Polymers. *Adv. Mater.* **2014**, *26*, 2993−2998.

(7) Zhang, W.; Han, Y.; Zhu, X.; Fei, Z.; Feng, Y.; Treat, N. D.; Faber, H.; Stingelin, N.; Mcculloch, I.; Anthopoulos, T. D.; Heeney, M. A Novel Alkylated Indacenodithieno[3,2-B]thiophene-Based Polymer for High-Performance Field-Effect Transistors. *Adv. Mater.* **2016**, *28*, 3922−3927.

(8) Lee, B. H.; Bazan, G. C.; Heeger, A. J. Doping-Induced Carrier Density Modulation in Polymer Field-Effect Transistors. *Adv. Mater.* **2016**, *28*, 57−62.

(9) Jones, B. A.; Facchetti, A.; Wasielewski, M. R.; Marks, T. J. Tuning Orbital Energetics in Arylene Diimide Semiconductors. Materials Design for Ambient Stability of N-Type Charge Transport. *J. Am. Chem. Soc.* **2007**, *129*, 15259−12529.

(10) Nicolai, H. T.; Kuik, M.; Wetzelaer, G. A. H.; de Boer, B.; Campbell, C.; Risko, C.; Brédas, J. L.; Blom, P. W. M. Unification of Trap-Limited Electron Transport in Semiconducting Polymers. *Nat. Mater.* **2012**, *11*, 882−887.

(11) Usta, H.; Risko, C.; Wang, Z.; Huang, H.; Deliomeroglu, M. K.; Zhukhovitskiy, A.; Facchetti, A.; Marks, T. J. Design, Synthesis, and Characterization of Ladder-Type Molecules and Polymers. Air-Stable, Solution-Processable N-Channel and Ambipolar Semiconductors for Thin-Film Transistors via Experiment and Theory. *J. Am. Chem. Soc.* **2009**, *131*, 5586−5608.

(12) Zhong, H.; Smith, J.; Rossbauer, S.; White, A. J. P.; Anthopoulos, T. D.; Heeney, M. Air-Stable and High-Mobility N-Channel Organic Transistors Based on Small-Molecule/polymer Semiconducting Blends. *Adv. Mater.* **2012**, *24*, 3205−3211.

(13) Anthopoulos, T. D.; Anyfantis, G. C.; Papavassiliou, G. C.; De Leeuw, D. M. Air-Stable Ambipolar Organic Transistors. *Appl. Phys. Lett.* **2007**, *90*, 122105.

(14) Sommer, M. Conjugated Polymers Based on Naphthalene Diimide for Organic Electronics. *J. Mater. Chem. C* **2014**, *2*, 3088−3098.

(15) Zhan, X.; Facchetti, A.; Barlow, S.; Marks, T. J.; Ratner, M. A.; Wasielewski, M. R.; Marder, S. R. Rylene and Related Diimides for Organic Electronics. *Adv. Mater.* **2011**, *23*, 268−284.

(16) Anthony, J. E.; Facchetti, A.; Heeney, M.; Marder, S. R.; Zhan, X. N-Type Organic Semiconductors in Organic Electronics. *Adv. Mater.* **2010**, *22*, 3876−3892.

(17) Tan, Z.; Zhou, E.; Zhan, X.; Wang, X.; Li, Y.; Barlow, S.; Marder, S. R. Efficient All-Polymer Solar Cells Based on Blend of Tris(thienylenevinylene)-Substituted Polythiophene and Poly[perylene Diimide-Alt-Bis(dithienothiophene)]. *Appl. Phys. Lett.* **2008**, *93*, 073309.

(18) Babel, A.; Jenekhe, S. A. High Electron Mobility in Ladder Polymer Field-Effect Transistors. *J. Am. Chem. Soc.* **2003**, *125*, 13656−13657.

(19) Mikroyannidis, J. A.; Stylianakis, M. M.; Sharma, G. D.; Balraju, P.; Roy, M. S. A Novel Alternating Phenylenevinylene Copolymer with Perylene Bisimide Units: Synthesis, Photophysical, Electrochemical, and Photovoltaic Properties. *J. Phys. Chem. C* **2009**, *113*, 7904−7912.

(20) Guo, X.; Watson, M. D. Conjugated Polymers from Napthalene Bisimide. *Org. Lett.* **2008**, *10*, 5333−5336.

(21) Hüttner, S.; Sommer, M.; Thelakkat, M. N-Type Organic Field Effect Transistors from Perylene Bisimide Block Copolymers and Homopolymers. *Appl. Phys. Lett.* **2008**, *92*, 093302.

(22) Zhan, X.; Tan, Z.; Zhou, E.; Li, Y.; Misra, R.; Grant, A.; Domercq, B.; Zhang, X.-H.; An, Z.; Zhang, X.; Barlow, S.; Kippelen, B.; Marder, S. R. Copolymers of Perylene Diimide with Dithienothiophene and Dithienopyrrole as Electron-Transport Materials for

DOI: 10.1021/acs.macromol.6b01423
Macromolecules XXXX, XXX, XXX−XXX

All-Polymer Solar Cells and Field-Effect Transistors. *J. Mater. Chem.* **2009**, *19*, 5794−5803.
(23) Zhan, X.; Tan, Z.; Domercq, B.; An, Z.; Zhang, X.; Barlow, S.; Li, Y.; Zhu, D.; Kippelen, B.; Marder, S. R. A High-Mobility Electron-Transport Polymer with Broad Absorption and Its Use in Field-Effect Transistors and All-Polymer Solar Cells. *J. Am. Chem. Soc.* **2007**, *129*, 7246−7247.
(24) Chen, Z.; Zheng, Y.; Yan, H.; Facchetti, A. Naphthalenedicarboximide- vs Perylenedicarboximide-Based Copolymers. Synthesis and Semiconducting Properties in Bottom-Gate N-Channel Organic Transistors. *J. Am. Chem. Soc.* **2009**, *131*, 8−9.
(25) Yan, H.; Chen, Z.; Zheng, Y.; Newman, C.; Quinn, J. R.; Dötz, F.; Kastler, M.; Facchetti, A. A High-Mobility Electron-Transporting Polymer for Printed Transistors. *Nature* **2009**, *457*, 679−686.
(26) Chen, H.; Guo, Y.; Mao, Z.; Yu, G.; Huang, J.; Zhao, Y.; Liu, Y. Naphthalenediimide-Based Copolymers Incorporating Vinyl- Linkages for High-Performance Ambipolar Field-Effect Transistors and Complementary-Like Inverters under Air. *Chem. Mater.* **2013**, *25*, 3589−3596.
(27) Kim, R.; Amegadze, P. S. K.; Kang, I.; Yun, H.-J.; Noh, Y.-Y.; Kwon, S.-K.; Kim, Y.-H. High-Mobility Air-Stable Naphthalene Diimide-Based Copolymer Containing Extended π-Conjugation for N-Channel Organic Field Effect Transistors. *Adv. Funct. Mater.* **2013**, *23*, 5719−5727.
(28) Guo, X.; Kim, F. S.; Seger, M. J.; Jenekhe, S. A.; Watson, M. D. Naphthalene Diimide-Based Polymer Semiconductors: Synthesis, Structure − Property Correlations, and N-Channel and Ambipolar Field-E Ff Ect Transistors. *Chem. Mater.* **2012**, *24*, 1434−1442.
(29) Huang, H.; Chen, Z.; Ortiz, R. P.; Newman, C.; Usta, H.; Lou, S.; Youn, J.; Noh, Y. Y.; Baeg, K. J.; Chen, L. X.; Facchetti, A.; Marks, T. Combining Electron-Neutral Building Blocks with Intramolecular "conformational Locks" affords Stable, High-Mobility P- and N-Channel Polymer Semiconductors. *J. Am. Chem. Soc.* **2012**, *134*, 10966−10973.
(30) Hwang, Y.-J.; Murari, N. M.; Jenekhe, S. A. New N-Type Polymer Semiconductors Based on Naphthalene Diimide and Selenophene Derivatives for Organic Field-Effect Transistors. *Polym. Chem.* **2013**, *4*, 3187−3420.
(31) Hwang, Y.; Ren, G.; Murari, N. M.; Jenekhe, S. A. n-Type Naphthalene Diimide−Biselenophene Copolymer for All- Polymer Bulk Heterojunction Solar Cells. *Macromolecules* **2012**, *45*, 9056−9602.
(32) Vasimalla, S.; Senanayak, S. P.; Sharma, M.; Narayan, K. S.; Iyer, P. K. Improved Performance of Solution-Processed N-Type Organic Field-Effect Transistors by Regulating the Intermolecular Interactions and Crystalline Domains on Macroscopic Scale. *Chem. Mater.* **2014**, *26*, 4030−4037.
(33) Zhang, X.; Xiao, C.; Zhang, A.; Yang, F.; Dong, H.; Wang, Z.; Zhan, X.; Li, W.; Hu, W. Pyridine-Bridged Diketopyrrolopyrrole Conjugated Polymers for Field-Effect Transistors and Polymer Solar Cells. *Polym. Chem.* **2015**, *6*, 4775−4783.
(34) Yuan, M.; Durban, M. M.; Kazarinoff, P. D.; Zeigler, D. F.; Rice, A. H.; Segawa, Y.; Luscombe, C. K. Synthesis and Characterization of Fused-Thiophene Containing Naphthalene Diimide N-Type Copolymers for Organic Thin Film Transistor and All-Polymer Solar Cell Applications. *J. Polym. Sci., Part A: Polym. Chem.* **2013**, *51*, 4061−4069.
(35) Fazzi, D.; Caironi, M.; Castiglioni, C. Quantum-Chemical Insights into the Prediction of Charge Transport with Enhanced Electron Mobility. *J. Am. Chem. Soc.* **2011**, *133*, 19056−19059.
(36) Schuettfort, T.; Huettner, S.; Lilliu, S.; Macdonald, J. E.; Thomsen, L.; Mcneill, C. R. Surface and Bulk Structural Characterization of a High- Mobility Electron-Transporting Polymer. *Macromolecules* **2011**, *44*, 1530−1539.
(37) Schuettfort, T.; Thomsen, L.; Mcneill, C. R. Observation of a Distinct Surface Molecular Orientation in Films of a High Mobility Conjugated Polymer. *J. Am. Chem. Soc.* **2013**, *135*, 1092−1101.
(38) Steyrleuthner, R.; Schubert, M.; Howard, I. A.; Klaumünzer, B.; Schilling, K.; Chen, Z.; Saalfrank, P.; Laquai, F.; Facchetti, A.; Neher, D. Aggregation in a High Mobility N-Type Low Bandgap Copolymer with Implications on Semicrystalline Morphology. *J. Am. Chem. Soc.* **2012**, *134*, 18303−18317.
(39) Luzio, A.; Fazzi, D.; Nübling, F.; Matsidik, R.; Straub, A.; Komber, H.; Giussani, E.; Watkins, S. E.; Barbatti, M.; Thiel, W.; Gann, E.; Thomsen, L.; Mcneill, C. R.; Caironi, M.; Sommer, M. Structure − Function Relationships of High-Electron Mobility Naphthalene Diimide Copolymers Prepared Via Direct Arylation. *Chem. Mater.* **2014**, *26*, 6233−6240.
(40) Fei, Z.; Pattanasattayavong, P.; Han, Y.; Schroeder, B. C.; Yan, F.; Kline, R. J.; Anthopoulos, T. D.; Heeney, M. Influence of Side-Chain Regiochemistry on the Transistor Performance of High-Mobility, All-Donor Polymers. *J. Am. Chem. Soc.* **2014**, *136*, 15154−15157.
(41) Fei, Z.; Gao, X.; Smith, J.; Pattanasattayavong, P.; Domingo, E. B.; Stingelin, N.; Watkins, S. E.; Anthopoulos, T. D.; Kline, R. J.; Heeney, M. Near Infrared Absorbing Soluble Poly(cyclopenta[2,1-b:3,4- B′]dithiophen-4-One)vinylene Polymers Exhibiting High Hole and Electron Mobilities in Ambient Air. *Chem. Mater.* **2013**, *25*, 59−68.
(42) Tremel, K.; Ludwigs, S.; Hufnagel, M.; Brinkmann, M.; Gonthier, E.; Sommer, M. Segregated versus Mixed Interchain Stacking in Highly Oriented Films of Naphthalene Diimide Bithiophene Copolymers. *ACS Nano* **2012**, *6*, 10319−10326.
(43) Durban, M. M.; Kazarinoff, P. D.; Luscombe, C. K. Synthesis and Characterization of Thiophene-Containing Naphthalene Diimide N-Type Copolymers for OFET Applications. *Macromolecules* **2010**, *43*, 6348−6352.
(44) Luzio, A.; Criante, L.; D'Innocenzo, V.; Caironi, M. Control of Charge Transport in a Semiconducting Copolymer by Solvent-Induced Long-Range Order. *Sci. Rep.* **2013**, *3*, 3425.
(45) Kim, Y.; Hong, J.; Oh, J. H.; Yang, C. Naphthalene Diimide Incorporated Thiophene-Free Copolymers with Acene and Heteroacene Units: Comparison of Geometric Features and Electron-Donating Strength of Co-Units. *Chem. Mater.* **2013**, *25*, 3251−3259.
(46) Szumilo, M. M.; Gann, E. H.; Mcneill, C. R.; Lemaur, V.; Oliver, Y.; Thomsen, L.; Vaynzof, Y.; Sommer, M.; Sirringhaus, H. Structure Influence on Charge Transport in Naphthalenediimide − Thiophene Copolymers. *Chem. Mater.* **2014**, *26*, 6796−6804.
(47) Matsidik, R.; Komber, H.; Luzio, A.; Caironi, M.; Sommer, M. Defect-free Naphthalene Diimide Bithiophene Copolymers with Controlled Molar Mass and High Performance via Direct Arylation Polycondensation. *J. Am. Chem. Soc.* **2015**, *137*, 6705−6711.
(48) Chen, Z.; Lee, M. J.; Shahid Ashraf, R.; Gu, Y.; Albert-Seifried, S.; Meedom Nielsen, M.; Schroeder, B.; Anthopoulos, T. D.; Heeney, M.; McCulloch, I.; Sirringhaus, H. High-Performance Ambipolar Diketopyrrolopyrrole-thieno[3,2-B]thiophene Copolymer Field-Effect Transistors with Balanced Hole and Electron Mobilities. *Adv. Mater.* **2012**, *24*, 647−652.
(49) Anthopoulos, T. D.; Setayesh, S.; Smits, E.; Cölle, M.; Cantatore, E.; De Boer, B.; Blom, P. W. M.; De Leeuw, D. M. Air-Stable Complementary-like Circuits Based on Organic Ambipolar Transistors. *Adv. Mater.* **2006**, *18*, 1900−1904.
(50) Anthopoulos, T. D.; Tanase, C.; Setayesh, S.; Meijer, E. J.; Hummelen, J. C.; Blom, P. W. M.; De Leeuw, D. M. Ambipolar Organic Field-Effect Transistors Based on a Solution-Processed Methanofullerene. *Adv. Mater.* **2004**, *16*, 2174−2179.
(51) Kim, N. K.; Khim, D.; Xu, Y.; Lee, S. H.; Kang, M.; Kim, J.; Facchetti, A.; Noh, Y. Y.; Kim, D. Y. Solution-Processed Barium Salts as Charge Injection Layers for High Performance N-Channel Organic Field-Effect Transistors. *ACS Appl. Mater. Interfaces* **2014**, *6*, 9614−9621.
(52) Sirringhaus, H. 25th Anniversary Article: Organic Field-Effect Transistors: The Path beyond Amorphous Silicon. *Adv. Mater.* **2014**, *26*, 1319−1335.

DOI: 10.1021/acs.macromol.6b01423
Macromolecules XXXX, XXX, XXX−XXX